Passive and Active Mixing in Microfluidic Devices

Han E.H. Meijer, Mrityunjay K. Singh, Tae Gong Kang, Jaap M.J. den Toonder, Patrick D. Anderson*

Summary: In microfluidics the Reynolds number is small, preventing turbulence as a tool for mixing, while diffusion is that slow that time does not yield an alternative. Mixing in microfluidics therefore must rely on chaotic advection, as well-known from polymer technology practice where on macroscale the high viscosity makes the Reynolds numbers low and diffusion slow. The mapping method is used to analyze and optimize mixing also in microfluidic devices. We investigate passive mixers like the staggered herringbone micromixer (SHM), the barrier embedded micromixer (BEM) and a three-dimensional serpentine channel (3D-SC). Active mixing is obtained via incorporating particles that introduce a hyperbolic flow in e.g. two dimensional serpentine channels. Magnetic beads chains-up in a flow after switching on a magnetic field. Rotating the field creates a physical rotor moving the flow field. The Mason number represents the ratio of viscous forces to the magnetic field strength and its value determines the fate of the rotor: a single, an alternating single and double, or a multiple part chain-rotor results. The type of rotor determines the mixing quality with best results in the alternating case where crossing streamlines introduce chaotic advection. Finally, an active mixing device is proposed that mimics the cilia in nature. The transverse flow induced by their motion indeed enhances mixing at the microscale.

Keywords: BEM; cilia; magnetic beads; serpentine; SHM

Introduction

Most of the efficient micro-mixers proposed in the last decade are based on pressure driven flows that include the baker's transformation as known from the working principle of static mixers frequently applied in different polymer processing operations. The mechanism to achieve effective mixing in laminar flows is that of repetitive stretching and folding and the low Reynolds and high Péclet numbers that are typically for micromixers, require application of this mechanism to obtain sufficient mixing. Essential is to generate a spatial-periodic alternating transversal flow. Different designs to achieve this are reviewed and optimized with as typical examples the staggered herringbone mixer and the barrier-embedded mixer. The last passive mixer dealt with is the 3D serpentine channel that only functions at Reynolds numbers larger than one. Sometimes a more active actuation may be desirable with the advantage that both flow and mixing can be controlled, i.e. ranging from almost no mixing from intermediate levels to complete mixing. Two different approaches of active mechanisms will be discussed: the first based on magnetic particles, the second on artificial cilia.

Mapping Method

The optimum design of any mixer represents the situation where a required mixing is achieved using a minimum amount of energy or pressure drop. The question is how to find the optimum geometry and

TU/e, P.O. Box 513. 5600 MB Eindhoven, The Netherlands
E-mail: h.e.h.meijer@tue.nl

CFD analyses for a large number of different geometries are usually not an attractive and efficient technique. The mapping method, which is based on an original suggestion by Spencer and Wiley,[1] is an elegant engineering approach to find this optimum. Anderson and Meijer,[2] Galaktionov *et al.* [3], and Kruijt *et al.* [4] successfully developed and utilized the mapping method to optimize macro-mixing devices like the lid-driven cavity flow and the Kenics static mixer. The original mapping method has been modified such that the coefficients of the mapping matrices can be computed in a simpler way, see Singh *et al.* [5]. The idea is as follows: *a distribution matrix* φ is formed to store information about the distribution of fluid from one cross-section to the next due to a specified flow. To define the coefficients of the distribution matrix, the initial cross section of the flow domain is subdivided into a large number N of discrete cells of identical size. During flow, the material from a donor cell is transferred to different recipient cells and the fraction of material that is transferred from the donor cell to a recipient cell gives the distribution coefficient of the donor cell with respect to that recipient cell. To approximate the coefficients of the mapping matrix a number of markers inside all cells are followed. To determine the final distribution of markers, the markers are advected during the flow from $y = y_0$ to $y = y_0 + \Delta y$, see Figure 1.

If the number of markers in the donor sub-domain number Ω_i is M_i at $y = y_0$ and the number of markers found after tracking in the recipient sub-domain number Ω_j is M_{ij} at $y = y_0 + \Delta y$, then the mapping coefficient Φ_{ij} is calculated as: $\Phi_{ij} = M_{ij}/M_i$. In other words the coefficient Φ_{ij} is the measure of the fraction of total flux of the sub-domain Ω_i donated to the sub-domain Ω_j. The elegance of the mapping approach is that if one wants to analyze mixing-related scalar quantities, like a concentration vector $C \quad IR^{I \times N}$ defined on the initial sub-domains, then the concentration evolution C^I after the deformation is simply obtained by multiplying the initial concentration vector C^0 with the mapping matrix Φ.

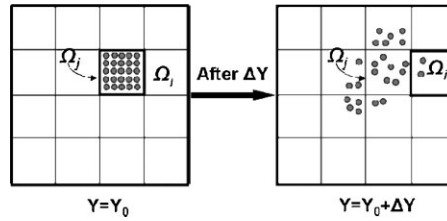

Figure 1.
Illustration of the computation of the coefficient Φ_{ij} in the mapping matrix Φ. The cell Ω_i at the initial cross-section $z = z_o$ is covered with markers that are tracked during flow in Δy (to arrive at the final cross section $y = y_o + \Delta y$). The ratio of the number of markers received by recipient cell Ω_j to initial number of markers of Ω_i is determined (in this example Φ_{ij} is 2/25).

Part 1: Passive Mixers

SHM

One of the most known static micro-mixers is the SHM, the staggered herringbone mixer, see e.g. Stroock *et al.* [6]. The mixer consists of two different basic units which both create a transversal flow consisting of two counter-rotating vortices. Material elements travelling down the mixer periodically go from one unit to the next, thus from one transversal flow to the next, and hence periodically stretch and fold. A complete analysis of mixing in the SHM is presented in Singh *et al.* [5] and here some main results are highlighted. To find the optimum design, the logarithm of discrete intensity of segregation versus pressure drop is plotted in Figure 2, which shows the results for SHMs with 6, 8, 10 and 14 numbers of grooves. From this plot it follows that the largest drop in intensity of segregation at a given pressure drop (vertical line in Figure 2), is found for 10 grooves per half cycle. Alternatively, a given mixing quality of e.g. $log_{10}\, I_d = -2.5$ (the horizontal line in Figure 2), is obtained

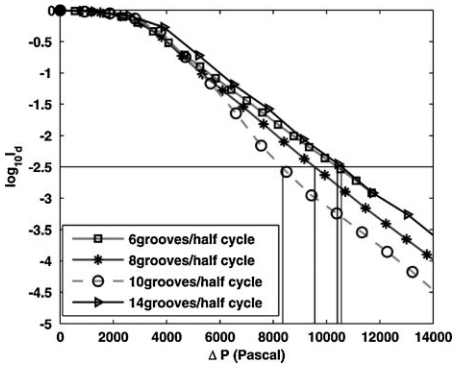

Figure 2.
The intensity of segregation versus pressure drop (up to 20th mixing cycle) for SHM designs with 6, 8, 10 and 14 grooves per half cycle. Clearly the optimum number of grooves is 10 given the lowest pressure drop (energy used) for the same mixing quality. From Singh *et al.* [5].

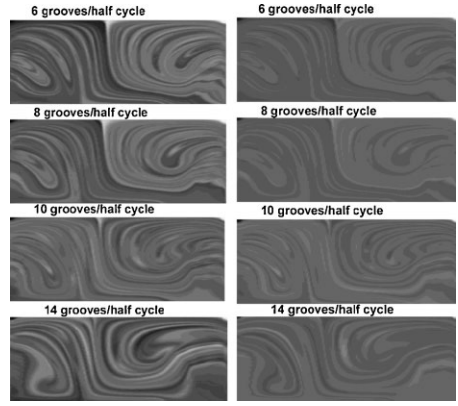

Figure 3.
Mixing patterns for different SHM designs: left images for the same pressure drop (vertical line Figure 2); right images for the same mixing quality (horizontal line in X2X). From Singh *et al.* [5].

with pressure drops close to 10439, 9503, 8353 and 10665 Pa (N/m^2), for SHMs with 6, 8, 10 and 14 grooves per half cycle, respectively, yielding the same optimum of 10 grooves. Clearly the optimum number of grooves is 10 given the lowest pressure drop (energy used) for the same mixing quality.

BEM

A variation of the staggered herring bone mixer is found in barrier-embedded mixers (BEM), see Figure 4.

The channel has grooves on the bottom surface and a barrier at the top, see e.g. Kim *et al.* [7]. Similar as for the SHM design, periodic units can be defined yielding alternating transversal flow, hopefully leading to chaotic mixing flows. Various combinations of two or more mixing sequences (functional modules) of the BEM provide numerous competitive designs.

Again the mapping method can be used as an efficient tool to analyze various layouts of these micro-mixers, see for a detailed analysis of mixing in different BEM geometries Kang *et al.* [8]. The resulting mixing patterns are plotted in Figure 5.

The optimization is shown in Figure 6: The protocol *P*32 shows the best performance.

3D Serpentines

As a last example of a passive microfluidic mixer we consider the three-dimensional serpentine channel mixing device. The basic building block is a ''C-shaped''

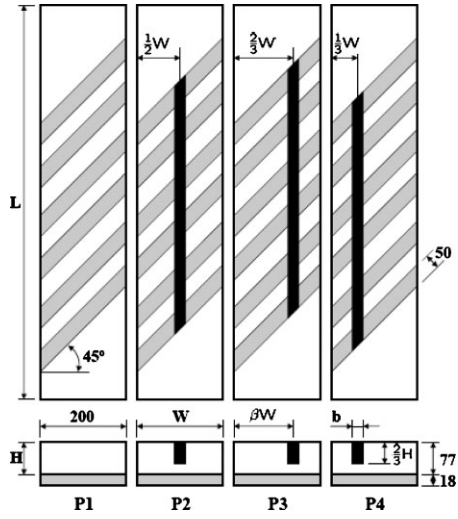

Figure 4.
The four basic BEM barrier-embedded mixing units. From Kang *et al.* [7].

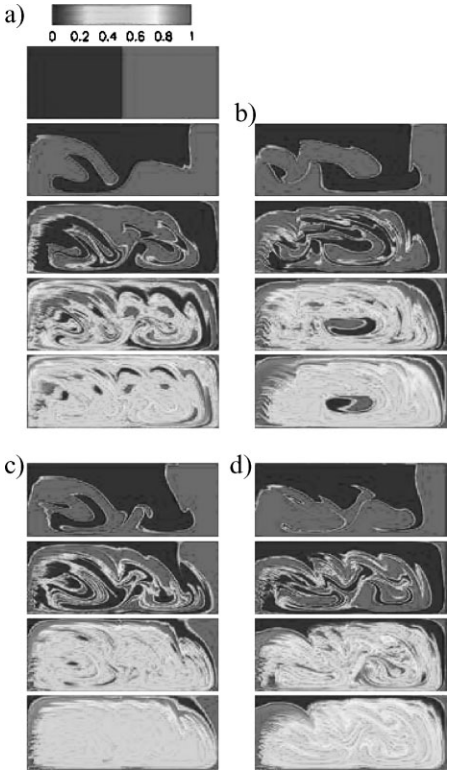

Figure 5.
Evolution of mixing patterns in the BEM at several down-channel positions, $y/L_c = 4$, 10, 20, and 30, for periodic sequences with Re = 0.01. The initial concentration at $y = 0$ is shown on the top; the color contours represent the spatial distribution of the concentration describing transport of the two fluids to be mixed. (a) P12, (b) P34, (c) P32, (d) P42 (from Kang *et al.* [8]).

section. Figure 7 shows the mixing evolutions along the down-channel positions after 1, 2, 3, 4, and 10 mixing cycles for Re = 0.01, 10, 50, and 70, see Singh *et al.* [8]. As the Reynolds number increases, stretching and folding of interfaces becomes more vigorous and it is evident that the flow at Re = 70 is capable of producing the best mixing, while in Stokes flow regime the flow is totally incapable to mix fluids.

Future research might consider novel serpentine channels where ''C-shaped'' sections are alternated with symmetry breaking modules. The mapping method could serve as an elegant technique to find the best design.

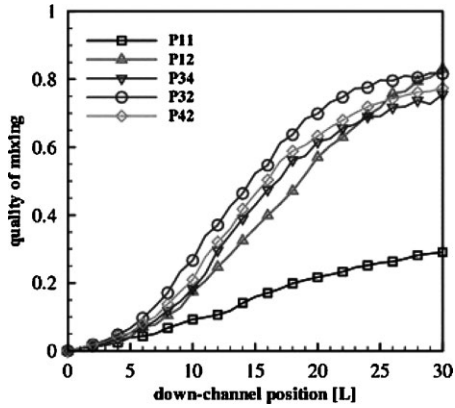

Figure 6.
Evolution of mixing quality Q (1-intensity of segregation) for five different periodic sequences (BEM mixer designs) versus the down-channel position y scaled by the length of one mixing protocol L_c (from Kang et al. [8]).

Part 2: Active Mixers

Results up to now demonstrate that by a clever design of channels effective mixing can result even in short mixing lengths. Of course one of the downsides of these passive channel designs is that they are primarily optimised for one Reynolds number or for a specific fluid combination with given rheological properties. If changes are induced to either the inlet velocity or the materials, a new (optimatized) design might

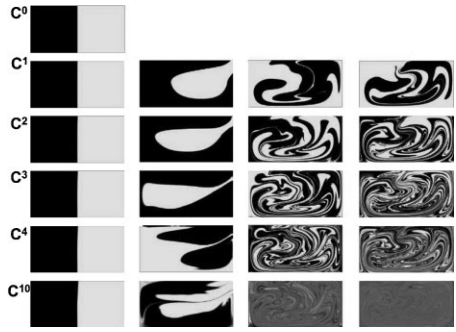

Figure 7.
Effect of Reynolds number on the evolution of mixing patterns in a serpentine channel at several down-channel positions after 1, 2, 3, 4, and 10 cycles of mixing. a) Re = 0.01, (b) Re = 10, (c) Re = 50, and (d) Re = 70 (from Singh *et al.* [5]).

be needed, which of course is possible, but also cumbersome. A more active approach to achieve mixing could therefore be more elegant and efficient. Here we discuss two prime example of routes to actively control mixing in microchannels or microchambers. The first is by using (magnetic) beads; the second is inspired by nature and artificical cilia are created which are activated to generate (transverse) flow and mixing.

2D Serpentines

Actuating a single particle in a 2D serpentine channel can introduce stretching and folding, see Figure 8. The particles are actuated via an external force in a sinusoidal manner perpendicular to the flow direction and once the force is sufficiently large, $F = 5$ in Figure 8, almost complete global chaos results as can be concluded from the Poincaré section:

Magnetic Beads

Next we consider the flow in a two-dimensional liquid-filled circular cavity with N paramagnetic particles, subjected to a rotating magnetic field, initially forming a chain aligned horizontally with its center at the cavity center. The string turns into a rotor once the magnetic field rotates and the Mason number, Ma, which is the ratio of viscous force to magnetic force under the influence of a rotating magnetic field, determines what happens.

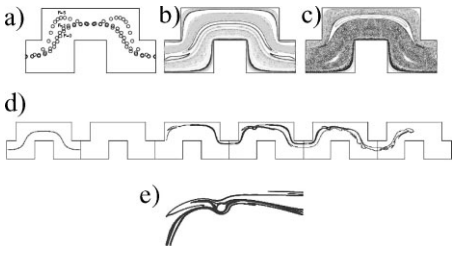

Figure 8.
Actuated single-particle problem. (a) Trajectories of particles for a force of the form, $F_x = 0$ and $F_y = F\ sin(4\pi x/L)$ with $F = 0$, 1 and 5, (b) Poincaré section for $F = 1$, (c) Poincaré section for $F = 5$, (d) deformation of a material strip, (e) detailed image showing stretching and folding around the rigid particle. From Kang *et al.* [9].

At a lower Mason number magnetic forces are dominant, while at a higher Mason number viscous forces are dominant. At low Mason numbers ($Ma < 0.001$) the chain formed acts as a single rotor, since it can follow the rotating magnetic field. At intermediate Mason numbers, the chain cannot follow the field, breaks up and may reform. Figure 9 shows the streamlines and chain configurations at the moment of chain break-up (left) and reformation (right) at $Ma = 0.002$. At chain break-up, hyperbolic flow is clearly observed and the deformed chain reveals a reverse S-like structure. Figure 10 shows the evolution in time of mixing in the cross section for different Mason numbers. From further analysis follows that optimal mixing is found for $Ma = 0.002$. As demonstrated, in that case the chain continuously breaks are reforms during rotation of the magnetic field.

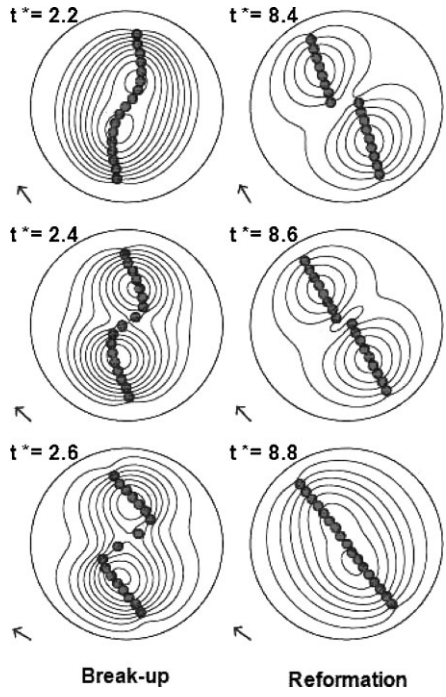

Figure 9.
Streamlines and chain configurations at the moment of chain break-up (left) and reformation (right) at $Ma = 0.002$. At chain break-up, hyperbolic flow is clearly observed and the deformed chain reveals a reverse S-like structure. From Kang *et al.* [10].

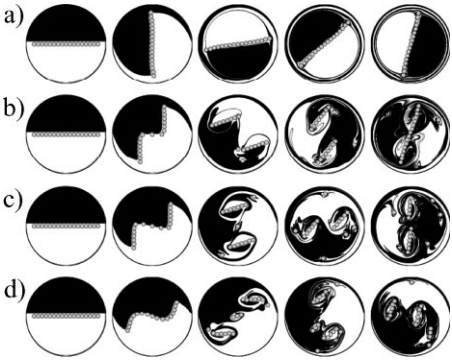

Figure 10.
Deformation of the interface between "black" and "white" fluids for the four Mason numbers, (a) Ma = 0.001, (b) Ma = 0.002, (c) Ma = 0.003, and (d) Ma = 0.005. The evolution of the deforming interface is plotted at the non-dimensional time $t^* = 0$, 2, 10, 20, and 30 (from left). From Kang *et al.* [10].

Artificial cilia

Finally, we discuss a design for an active mixer that is inspired by nature, specifically by the motion of ciliated or flagellated micro-organisms such as *E. coli* or *Paramecium*, see Figure 11. Cilia and flagella are microscopic hairs attached to the surface of the micro-organisms, which are rotated (flagella) or exhibit beating cycles (cilia) induced by molecular motors embedded in the cell membrane. This movement results in the propulsion of the micro-organism through the surrounding fluid. Typical lengths of the flagella and cilia are in the order of tens of micrometers, whereas the beating or rotation frequency ranges from 10 to 100 Hz.

By covering the microchannel walls with arrays of individually addressable artificial cilia in the form of micro-actuators, that are responsive to an external stimulus such as an electric or a magnetic field, flow and mixing is possible. These microactuators, with sizes similar to those of natural cilia, can be manufactured from polymer-based materials using micro-systems technologies. As shown in Figures 12 and 13 effective mixing by chaotic advection can be obtained with cilia-like microactuators integrated in a microfluidic channel. The results show that with a well-chosen geometrical arrangement and actuation scheme, exponential mixing can be obtained even with only two microactuators operating with a phase shift of $\varphi = \pi/2$ and placed on a distance equal to the length of the actuators.

Conclusions

The principles of efficient mixing in laminar flows, which are repetitive stretching and folding (and followed by bringing back to the original position), lead to chaotic advection also in the micro-channels of microfluidic devices. Of course limitations exist in the design choice of geometrical complexity, and alternative routes to induce asymmetric transverse flows that alternate and therefore lead to crossing streamlines, a prerequisite for exponential stretching in periodic hyperbolic points, had to be, and are, found. Both the

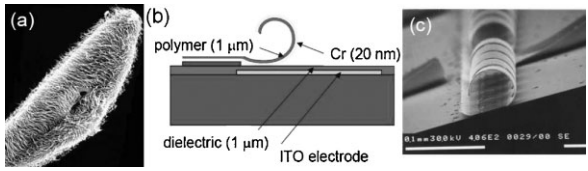

Figure 11.
(a) Paramecium: a micro-organism that makes use of beating cilia on its surface for propulsion. Its cross section is about 40 μm. (b) Cross-sectional sketch of artificial cilium. It is actuated by applying a voltage difference between the ITO electrode and the Cr film, upon which the cilium rolls out. After switching off the voltage, it rolls back by elastic recovery. (c) Electron micrograph showing the artificial cilia that have a length of 100 μm and a width of 20 μm.

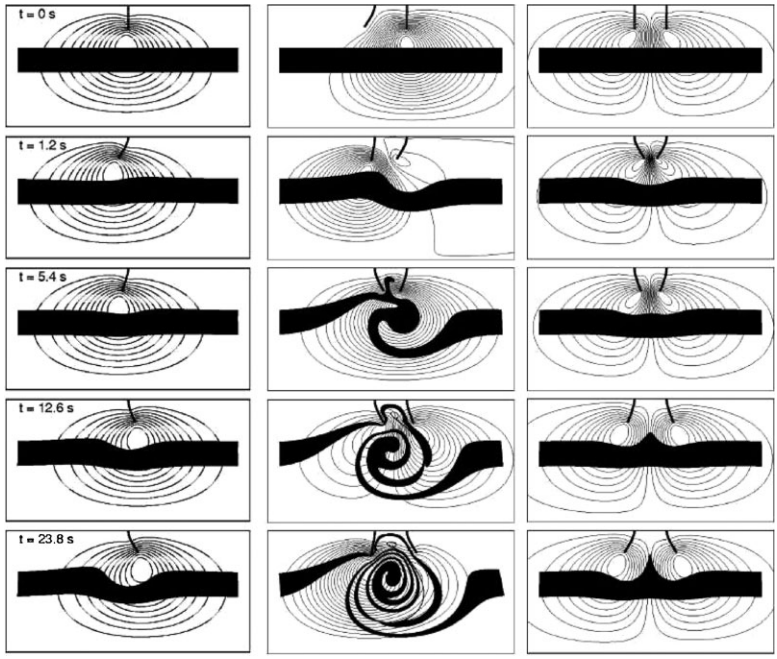

Figure 12.
Mixing analysis demonstration the effect of interplay of cilia. The left column shows the deformation pattern, the deformation of the black strip, for a single cilia. The middle and right column for two cilia moving at different phases. A phase shift of appears $\varphi = \pi/2$ to be optimal. From Khatavkar *et al.* [11].

staggered herringbone, SHM, and the barrier-embedded, BEM, mixer designs represent elegant solutions for improving mixing in low Reynolds number flows. For intermediate Reynolds number flows secondary flows driven by centrifugal forces can generate transverse velocities, e.g. the Dean flow in curved channels, resulting in efficient mixing. A prime example of such a geometry is the 3D serpentine channel. Dynamical tools to analyze chaotic advection in microfluidics are as useful as in macromixers. But also in microfluidics, only an engineering tool as the *mapping method* allows performing a large number of mixing computations in a very fast way, thus giving the tool to optimize mixing geometries or mixing protocols. Here this method is used to analyze and optimize the most widely used passive mixer designs.

Although rotors, stirrers, gears and screws are difficult to fabricate in the small dimensions of micro-channels, next to simplified passive mixer geometries also dynamic mixers have recently been proposed, driven by external fields. The presence of a few hard particles that basically replace the islands in periodic chaotic advection flows around which the material elements fold after being stretched. Moving beads effectively introduce a hyperbolic flow in their direct surroundings, stimulating mixing. Although interesting, also from a fundamental point of view, more applications of particles can be explored if they can be manipulated from the outside of the microfluidic device with one or another force field. As such, particles oscillating perpendicular to the Poiseuille flow in a two-dimensional, flat, serpentine channel indeed can induce the stretching and folding mechanism.

Magnetic beads randomly distributed in the flow automatically chain-up after switching on a magnetic field. The chain connects opposite boundaries of the mixing chamber and comprises a rotor, once the field starts rotating. The Mason number

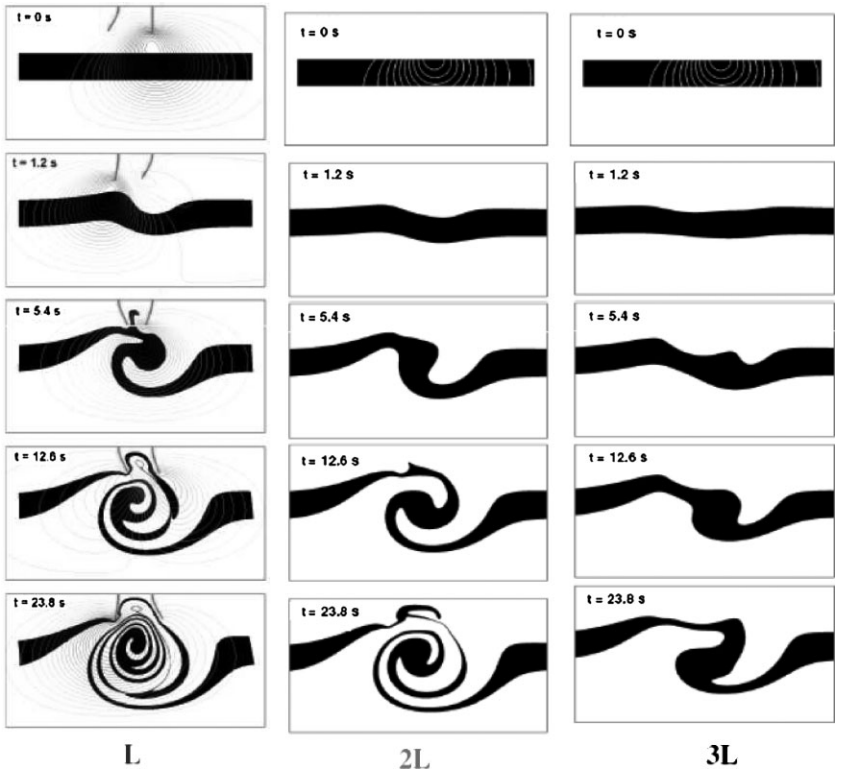

Figure 13.
Optimizing the distance between the actuators. A distance equal to the length of the actuators is optimal. From Khatavkar *et al.* [11].

gives the ratio of magnetic to viscous forces. At low Mason numbers, the rotor follows the magnetic field, a rather boring velocity field results with poor mixing. At intermediate Mason numbers, the chain cannot completely follow the rotation, breaks-up in two smaller chains that rotate independently for some time prior to reform into a single (S-curved) chain again, where after the procedure repeats. Interesting velocity fields result with one or two vortices and lead to crossing streamlines, to chaotic advection and, ultimately, in exponential mixing. At even higher Mason numbers, no recombination is possible, two (or three) independent rotors keep stirring the fluid, but with less efficiency because of lack of precise crossing streamlines and periodicity.

The last dynamic mixing principle tries to mimic the cilia in nature that result in a propelling motion. Tiny moveable flaps are mounted on the surface of the mixing chamber and their motion is controlled by an external field. Their length, relatively to the channel depth, their mutual distance, that should be far enough to allow independent motion but also sufficiently close to result in crossing streamlines, and the phase-lag of their motion, determine whether stretching and folding can be introduced to greatly enhance mixing in microfluidic devices.

[1] R. Spencer, R. Wiley, *Journal of Colloid Science* **1951**, *6*, p. 133–145.
[2] P. D. Anderson, H. E. H. Meijer, *Applied Rheology* **2000**, *10*(3), p. 119–133.
[3] O. S. Galaktionov, P. D. Anderson, G. W. M. Peters, H. E. H. Meijer, *Int. Polym. Proc.* **2003**, *XVII*(2), p. 138–150.

[4] P. G. M. Kruijt, O. S. Galaktionov, P. D. Anderson, G. W. M. Peters, H. E. H. Meijer, *AIChE J.* **2001**, *47*(5), p. 1005–1015.
[5] M. K. Singh, T. G. Kang, H. E. H. Meijer, P. D. Anderson, The mapping method as a toolbox to analyze, design, and optimize micromixers. Microfluidics and nanofluidics, online, **2008**.
[6] A. D. Stroock, S. K. Dertinger, A. Ajdari, H. A. Stone, G. M. Whitesides, *Science* **2002**, *295*, p. 647–651.
[7] D. S. Kim, S. W. Lee, T. H. Kwon, S. S. Lee, *J. Micromech. Microeng.* **2004**, *14*, p. 798–805.
[8] T. G. Kang, M. K. Singh, P. D. Anderson, T. H. Kwon, Chaotic mixing using periodic and aperiodic sequences of mixing protocols in a micromixer. Microfluidics and Nanofluidics, online **2008**.
[9] T. G. Kang, M. A. Hulsen, P. D. Anderson, Toonder, J. M. J. den, H. E. H. Meijer, *Chem. Eng. Sci.* **2007**, *62*(23), p. 6677–6686.
[10] T. G. Kang, M. A. Hulsen, Toonder, J. M. J. den, P. D. Anderson, H. E. H. Meijer, *Phys. Rev. E.* **2007**, *76*, 066303.
[11] V. Khatavkar, P. D. Anderson, Toonder, J. M. J. den, H. E. H. Meijer, *Phys. Fluids* **2007**, *19*, 083605.

